Journal of Materials Chemistry B

ROYAL SOCIETY OF CHEMISTRY

PAPER

View Article Online
View Journal | View Issue

Cite this: J. Mater. Chem. B, 2026, 14, 5769

Rapid detection and strain-level identification of milk-borne bacteria using a polymer-based chemical tongue

Kanako Takahashi,[a] Hiroyuki Kusada,[b] Hideyuki Tamaki,[b] Ryoji Kurita[ac] and Shunsuke Tomita*[ad]

Received 4th July 2025,
Accepted 13th April 2026

DOI: 10.1039/d5tb01573a

rsc.li/materials-b

The detection and strain-level identification of bacteria in food are critical for public health; however, conventional methods typically require expensive equipment, lengthy protocols, and/or specialized expertise. Here, we report a 'chemical tongue' strategy, *i.e.*, an analytical approach inspired by the human gustatory system, for the rapid and user-friendly strain-level sensing of foodborne bacteria. In this platform, a panel of cationic polymers that bear environment-responsive dansyl fluorophores interact nonspecifically yet differentially with the negatively charged bacterial surface, generating strain-specific fluorescence response patterns. By applying pattern-recognition algorithms, we accurately discriminated seven *Escherichia coli* (*E. coli*) strains. We further demonstrate the practical applicability of this approach to bacterial analysis in milk by integrating a brief and effective pretreatment that suppresses matrix-derived interference. This enables reliable strain-level identification across different milk matrices, discrimination of *E. coli* strains in the presence of spoilage-associated psychrotrophic bacteria, and time-dependent monitoring of milk quality changes induced by bacterial growth. Taken together, our chemical-tongue platform provides a rapid and cultivation-free solution for strain-level analysis of microbial contamination in complex food matrices, offering a promising foundation for next-generation food quality monitoring and safety management.

Introduction

Microorganisms inhabit virtually every environment and play vital roles in human life. Although helpful bacteria are harnessed for the production of valuable substances such as fermented foods[1] and pharmaceuticals,[2] pathogenic bacteria cause infectious diseases.[3] The characteristics of bacteria varies not only between species, but also within species; for example, while most *Escherichia coli* (*E. coli*) bacteria are safe and suitable for research or industrial use, some isolates can cause serious infections. These different effects can be attributed in part to variation at the strain level, where a bacterial strain is a clonal population derived from a single isolate. Although the various strains of a species generally share the same genetic background, subtle mutations can lead to distinct characteristics, including differences in pathogenicity, metabolic activity, and other functional traits.

In the food industry, the detection of bacteria is essential for ensuring product quality, assessing sanitary conditions, and preventing foodborne illnesses.[4] Many countries have established strict regulatory standards for permissible levels of pathogenic and non-pathogenic bacteria in food products. *E. coli* is widely used as an indicator of food contamination;[5] strains such as O157:H7 and O104:H4 cause severe disease in humans and animals, even at low doses, and have been implicated in foodborne outbreaks.[6,7] Therefore, identifying not only the bacterial species, but also the specific strains present, is increasingly important for understanding contamination status and supporting food safety, quality control, and agricultural monitoring.[8–10]

Currently, the detection and identification of bacterial strains rely on a combination of culture-based and molecular methods. In culture-based approaches, colony formation is observed on selective media, and species or strains are identified through morphological and biochemical analyses (*e.g.*, gram staining and enzymatic assays). In contrast, molecular methods, such as 16S rRNA sequencing[11] and matrix-assisted laser desorption/ionization time-of-flight mass spectrometry (MALDI-TOF MS),[12] enable

[a] Health and Medical Research Institute, National Institute of Advanced Industrial Science and Technology (AIST), 1-1-1 Higashi, Tsukuba, Ibaraki 305-8566, Japan. E-mail: s.tomita@aist.go.jp
[b] Biomanufacturing Process Research Center, AIST, 1-1-1 Higashi, Tsukuba, Ibaraki 305-8566, Japan
[c] Faculty of Pure and Applied Sciences, University of Tsukuba, 1-1-1 Tennodai, Tsukuba, Ibaraki 305-8573, Japan
[d] School of Integrative and Global Majors, University of Tsukuba, 1-1-1 Tennodai, Tsukuba, Ibaraki 305-8577, Japan

the precise identification through a highly sensitive analysis of genetic information. However, the expensive equipment and/or considerable time, labor, and specialized expertise required for these techniques limit their applicability in clinical and food-production settings, where rapid and cost-effective identification is desired.

To address this gap, we propose a strategy that integrates a panel of fluorogenic molecular probes with pattern-recognition algorithms. The diverse affinity levels of the molecular probes toward the unique features of the samples yield optical-pattern information that can be analyzed using pattern-recognition techniques. As this technology mimics the mechanism of human taste, it is often referred to as a "chemical tongue".[13–15] In many cases, merely mixing the molecular probes and sample followed by spectroscopic measurement is required, making the method both convenient and rapid and allowing for comparative analyses even when the sample composition is unknown. To date, chemical tongues have been used for the analysis of a variety of complex biological samples, including cells,[16–18] biofluids,[19,20] and beverages,[21–24] as well as for microbial analyses including the identification of isolated bacterial species[25–29] and the studies of biofilms[30,31] and microbiota.[32,33] Although chemical tongues have recently been extended to the identification of bacterial species in food matrices,[34–36] reports of strain-level discrimination remain scarce. Very recently, Zhang *et al.* have developed a multimodal sensor array that records plasmonic nanomaterial responses using four modalities [*i.e.*, surface-enhanced Raman scattering (SERS), UV-vis absorbance, dynamic light scattering (DLS), and ζ-potential], which led to the successful discrimination of *E. coli* strains in raw meat.[37] Such sensor platforms feature excellent accuracy and quantitative capabilities; however, further simplification and cost reduction are required to achieve the "mix-and-read" convenience, speed, and affordability needed for routine on-site use.

In this study, we have developed a chemical tongue for the rapid and simple identification of bacterial strains *via* a single fluorescence measurement. Milk was chosen as the target food due to its high susceptibility to microbial contamination during the handling of the raw material and manufacturing processes. Contamination of commercial milk with *E. coli*, lactic-acid bacteria, or psychrotrophic bacteria can result in milk spoilage,[38] and outbreaks of food poisoning caused by pathogenic bacteria such as certain *E. coli* strains remain a major societal problem.[6,7,39] Consequently, technologies that enable both the detection and identification of bacterial strains are in high demand.[38] Herein, we demonstrate that a chemical tongue composed of cationic polymers that bear environmentally sensitive dansyl (Dnc) moieties enables accurate strain-level discrimination and concentration-dependent response profiling of bacterial strains in contaminated milk (Fig. 1A). The Dnc-polymers were designed to maximize interaction diversity with minimal synthetic complexity by varying polymer-backbone size, conformation, and rigidity while maintaining a common fluorogenic motif. Because this chemical tongue offers a rapid and user-friendly means of strain-profiling without requiring microbial cultivation or genomic analysis, it holds promise for the development of practical sensing systems for food-quality monitoring and -safety assessment.

Experimental section

Materials and synthesis

Poly-L-lysine trifluoroacetate (PLL; degree of polymerization: 10, 55, and 258) and methoxy-poly(ethylene glycol)-*block*-PLL trifluoroacetate (PEG-*b*-PLL; degree of polymerization PEG: 113; degree of polymerization PLL: 52) were obtained from Alamanda Polymers, Inc. Polyamidoamine (PAMAM) dendrimer (generation 4.0), 3-morpholinopropanesulfonic acid (MOPS), and 2-morpholinoethanesulfonic acid (MES) were obtained from Sigma Chemical Co. Dansyl chloride (Dnc-Cl) was obtained from Tokyo Chemical Industry Co., Ltd. Polymers modified with dansyl chloride (Dnc-polymers) were prepared according to literature procedures,[40] as detailed in the SI.

Preparation of bacterial samples

All *E. coli* strains and *Acinetobacter bauminnii* (*A. bauminnii*) were purchased (see Table 1) and cultivated as described elsewhere. In brief, bacterial strains were grown overnight at 37 °C in Luria–Bertani medium while shaking at 200 rpm. Cell densities were measured as the optical density at 600 nm (OD_{600}) using a Nanodrop 2000c spectrophotometer (Thermo Fisher Scientific) and as colony-forming units (CFU mL^{-1}), which were determined by serial dilution of the bacterial suspensions, plating on Luria–Bertani agar plates, incubation at 37 °C overnight, and subsequent colony counting. The cells were stored at −80 °C until use. For the experiments reported in this study, bacterial samples were prepared from pre-cultured and stored stocks prepared under identical conditions. Prior to the study, the stock solution of the cells was thawed at 37 °C and centrifuged at 8000*g* (4 °C, 10 min). The supernatant was removed, and distilled water was added. This procedure was repeated twice. For spiking milk with the bacterial strains, solutions were prepared by mixing 0.3 mL of each of the bacterial strains with 3 mL of commercially available pasteurized milk. Next, 11.7 mL of solutions containing 0 or 64.1 mM of buffer [MES (pH = 5.7) or MOPS (pH = 7.0)], and 0 or 256 mM NaCl, were added. After allowing the mixture to stand for 10 min at room temperature, it was centrifuged at 8000*g* (4 °C, 10 min). The supernatant was removed, and this procedure was repeated once more. Finally, the sample was washed twice with distilled water.

For spoilage-monitoring experiments using *A. baumannii*, bacterial cells were cultured in Luria–Bertani medium and the cell density was determined as described above. Milk samples were then either spiked with *A. baumannii* at an initial concentration of OD_{600} = 0.001 or left unspiked as controls. The samples were incubated statically at 30 °C, and aliquots were collected daily. Each sample collected was subjected to the same pretreatment and fluorescence measurement procedures as described above.

Fluorescence responses of the polymers

Fluorescence measurements were performed using a BioTek Synergy H1 instrument (Agilent Technologies). Solutions (60 μL) containing 2.0 μg mL^{-1} of the Dnc-polymer and the

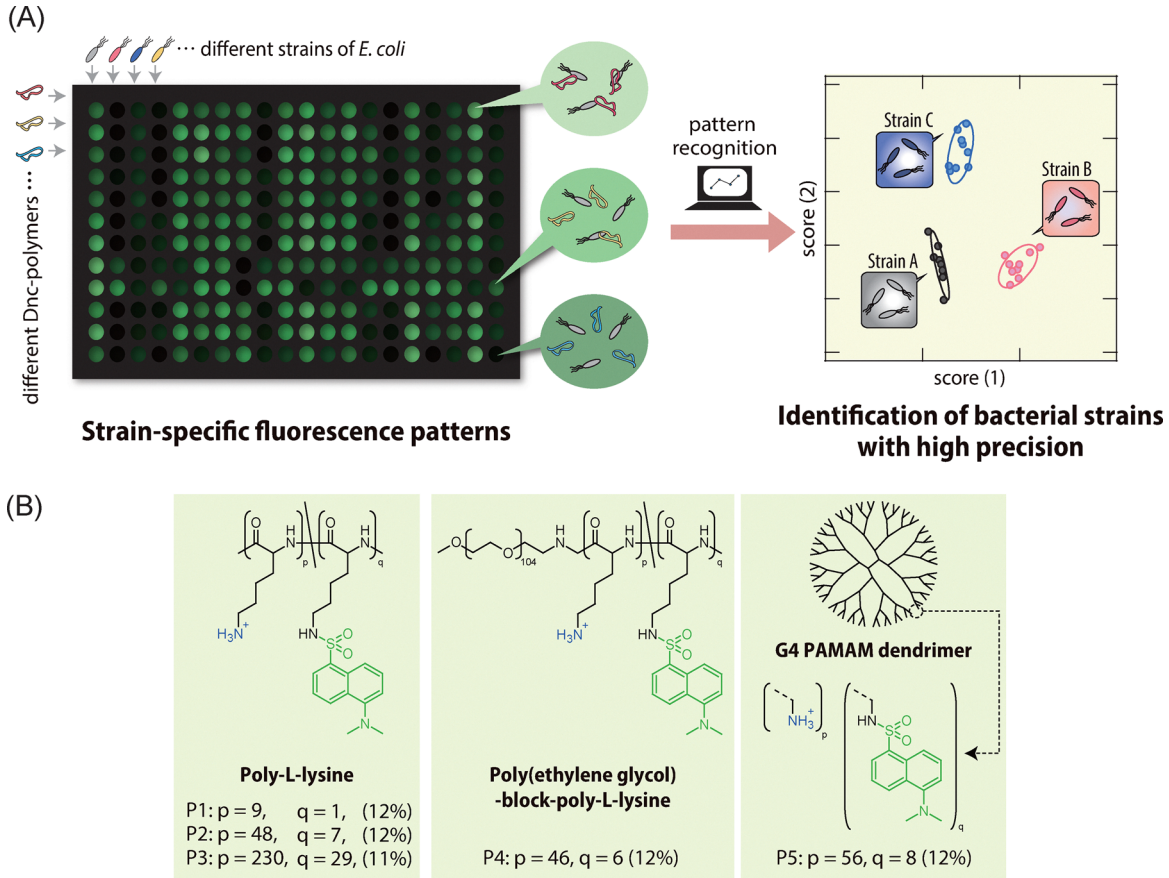

Fig. 1 Workflow and synthetic library for the optical-pattern recognition of bacterial strains. (A) Bacterial strain samples are analyzed using a chemical tongue composed of Dnc-polymers to generate fluorescence response patterns that reflect strain-specific characteristics, which are subsequently statistically analyzed using pattern-recognition algorithms. (B) Molecular structures of the cationic polymers modified with environmentally responsive Dnc fluorophores. Parentheses indicate the ratio of Dnc modification of the primary amines.

Table 1 Bacterial strains used in this study

Strain name	Abbr.	Source
E. coli		
JM109	*E.C.1*	TaKaRa
BL21(DE3) pLysS	*E.C.2*	BioDynamics Laboratory
Rosetta™ 2(DE3)	*E.C.3*	Merck Millipore
Origami™ 2(DE3)	*E.C.4*	Merck Millipore
Top10	*E.C.5*	Thermo Fisher Scientific
Rosetta-gamiB (DE3)	*E.C.6*	Merck Millipore
EPI300	*E.C.7*	Epicentre
A. baumannii		
NBRC 110491	*A.B.*	NITE Biological Resource Center

E. coli strain (OD_{600} = 0–0.25) in 20 mM MOPS buffer (pH = 7.0) and 150 mM NaCl were prepared in each well of a 384-well NBS™ black microplate (Corning Inc.) using a liquid-handling system (Assist Plus, Integra Biosciences). After incubation (35 °C, 10 min), the fluorescence spectra ($\lambda_{ex}/\lambda_{em}$ = 340 nm/402–700 nm) or fluorescence intensity ($\lambda_{ex}/\lambda_{em}$ = 340 nm/520 nm) were recorded at 35 °C.

Chemical-tongue sensing

Aliquots (48 μL) of solutions containing the Dnc-polymer (2.5 μg mL^{-1}) and 187.5 mM NaCl in 25 mM MOPS buffer (pH = 7.0) or 25 mM acetate buffer (pH = 5.0) were deposited in the wells of a 384-well plate using the liquid-handling system. After incubation (35 °C, 10 min), the fluorescence intensity was recorded using two different channels (Ch1: $\lambda_{ex}/\lambda_{em}$ = 330 nm/480 nm; Ch2: $\lambda_{ex}/\lambda_{em}$ = 360 nm/530 nm). For each condition, the fluorescence intensity was measured five times per well, and the averaged value was used for subsequent analysis. Subsequently, aliquots (12 μL) of the samples were added to each well, and the fluorescence intensity was recorded after incubation (35 °C, 10 min). These processes were performed at least six times for different samples to generate a training-data matrix. This training-data matrix was processed using linear discriminant analysis (LDA) in SYSTAT 13 (Systat Inc.). Each feature in the resulting data matrix corresponds to a specific polymer × pH × fluorescence channel combination, yielding a total of 5 polymers × 2 pH values × 2 channels as input variables for the LDA.

Results and discussion

Design of fluorescent polymer probes

The surfaces of *E. coli* comprise phospholipids and lipopolysaccharides, which leads to a negative overall charge. Accordingly,

cationic polymers capable of engaging in multivalent electrostatic interactions are particularly suited as scaffold molecules to acquire optical information through binding of the probes to the microbial surfaces. In this study, to obtain a panel of molecular probes capable of multifaceted bacteria recognition with minimal synthetic effort, we selected five cationic polymers (Fig. 1B): three types of PLL with different repeating units (**P1**, **P2**, and **P3**), a block copolymer of PLL and PEG (**P4**), and a PAMAM dendrimer (**P5**), thereby introducing diversity in polymer-backbone size, conformation, and rigidity. **P1**, **P2**, and **P3** are expected to yield different interaction profiles with bacterial surfaces due to their differences in size, which determine the accessible surface area and spatial resolution of interactions. The PEG segment in **P4** is thought to inhibit secondary aggregation by preventing polymer-bacteria complexes from further clustering with each other, which may lead to how densely bacterial cells pack together, resulting in a unique interaction mode compared to other polymers. In contrast, **P5**, being spherical and highly rigid, is anticipated to provide more pinpoint local surface information compared to the other flexible linear polymers.

To convert the interaction information with *E. coli* into a fluorescence signal, we introduced environmentally responsive Dnc groups onto a fraction of the primary amines of each polymer. We have previously used Dnc-modified fluorescent polymers for the construction of chemical tongues for proteins,[41] cells,[42] and culture media.[40] While Dnc groups exhibit weak fluorescence in aqueous environments, binding to proteins[41] or cells[42] results in a local decrease in polarity, which enhances the fluorescence intensity and shifts the emission peak. In addition, their large Stokes shift can effectively suppress background fluorescence.[43] In this manner, the five cationic Dnc-polymers with differing backbone structure and size can interact differently with the surface of *E. coli*, producing distinct fluorescence patterns. The Dnc modification ratio (~10% of amino groups) was selected based on a previous optimization, balancing sufficient fluorescence responsiveness with polymer solubility and suppression of spontaneous self-association.[42] We hypothesized that this would enable the identification of even subtle differences among *E. coli* strains (Fig. 1A).

Evaluation of the responses of the Dnc-polymers to *E. coli*

To evaluate the responsiveness of the designed polymers to *E. coli*, we first examined the fluorescence changes upon mixing two different *E. coli* strains (*E.C.*3 and *E.C.*7; Table 1) with either the linear polymer **P2** or the globular polymer **P5** (Fig. 2).

As the concentration of *E. coli* was increased, the fluorescence intensity of **P2** increased, accompanied by a notable blue shift of the emission peak (Fig. 2A). This response is likely due to a change in the polarity around the Dnc moiety upon the binding of **P2** to the bacterial surface. The fluorescence intensity for all Dnc-polymer/strain combinations increased with the microbial concentration up to OD_{600} = 0.12 and then plateaued (Fig. 2B). For reference, response curves plotted as the fluorescence intensity as a function of CFU mL^{-1}, together with the corresponding linear range, limit of detection (LoD), and limit of quantification (LoQ) are provided in Fig. S1. Notably, both Dnc-polymers showed greater maximum fluorescence intensity in response to the strain *E.C.*7, suggesting that the Dnc-polymers can capture strain-specific differences with respect to surface properties. Furthermore, **P2** showed a stronger fluorescence response to both *E. coli* strains, possibly due to the smaller effective interaction area of rigid, globular **P5** compared to that of flexible, linear **P2**. A similar trend was observed at pH = 5.0 (Fig. S2). Thus, the Dnc-polymers in this study exhibit strain-dependent variations in fluorescence response, which is desirable for the fluorescence-pattern-based sensing of bacterial strains.

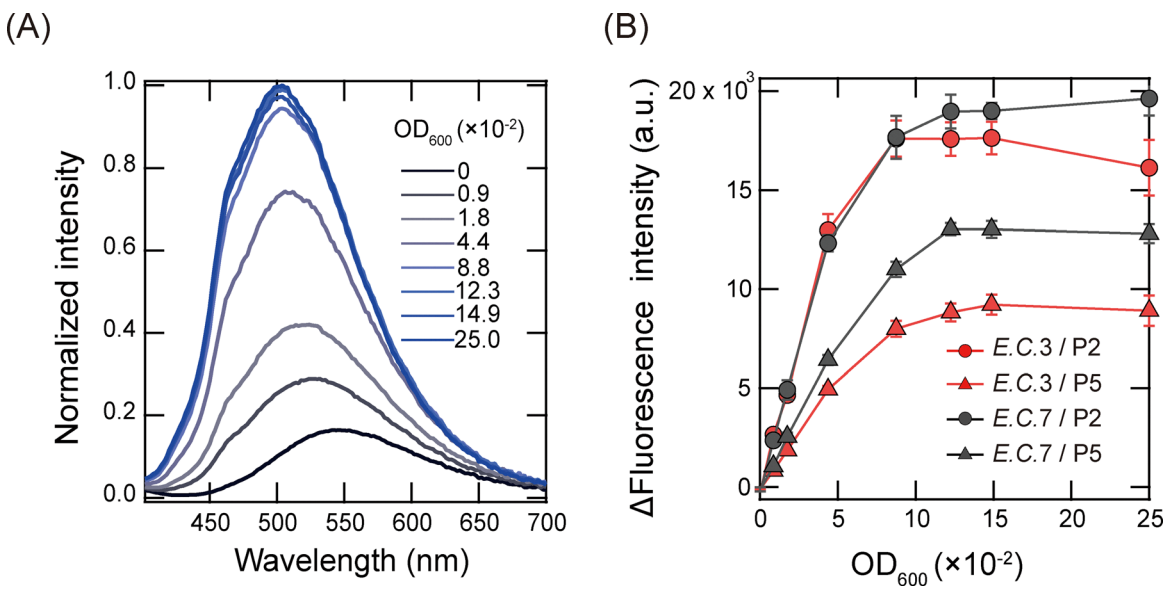

Fig. 2 Characterization of representative Dnc-polymers. (A) Fluorescence spectra of **P2** (20 μg mL^{-1}) upon addition of *E.C.*7 (OD_{600} = 0–0.25) in 20 mM MOPS buffer (pH = 7.0); λ_{ex} = 340 nm. (B) Binding isotherms for **P2** and **P5** (20 μg mL^{-1}) upon addition of *E.C.*3 and *E.C.*7 in 20 mM MOPS buffer (pH = 7.0); $\lambda_{ex}/\lambda_{em}$ = 340 nm/520 nm. The values shown represent mean values ± 1 SE from three independent experiments.

Strain-level discrimination

Having confirmed that the Dnc-polymers exhibit strain-dependent turn-on responses toward *E. coli*, we next attempted the discrimination of the seven *E. coli* strains (Table 1) based on their fluorescence-response patterns. Briefly, all possible combinations of each *E. coli* strain (OD_{600} = 0.10) with each Dnc-polymer (2.0 μg mL^{-1}) in 20 mM buffer (pH = 7.0 or 5.0) were prepared on a 384-well microplate. The fluorescence intensity of each bacteria/polymer/buffer combination was measured using two excitation/emission wavelength pairs (Ch1: $\lambda_{ex}/\lambda_{em}$ = 330 nm/480 nm; Ch2: $\lambda_{ex}/\lambda_{em}$ = 360 nm/530 nm). This yielded a dataset of fluorescence-intensity changes before and after sample addition (I–I_0) for 7 strains × 5 polymers × 2 pH values × 2 channels. Because the ionization states of the charged residues on the *E. coli* membrane (*e.g.*, carboxyl and phosphate groups) are pH-dependent, the use of different pH conditions enhances the capture of strain-specific surface characteristics.[33] In addition, polarity changes not only enhance the fluorescence intensity of Dnc, but also induce shifts in its emission peak; therefore, detection at multiple wavelengths provides more comprehensive information.[41]

The resulting heatmap of fluorescence responses exhibited diverse patterns depending on the strain (Fig. 3A and Dataset S1). Notably, **P5** at pH = 7.0 showed relatively lower responses to *E.C.*3 and *E.C.*6 than the other four Dnc-polymers. Although the rigid dendrimeric structure of **P5** may limit its effective interaction with bacterial surfaces, the precise strain-specific origin of this behavior is not yet fully understood. Furthermore, while the responses to *E.C.*6 and *E.C.*2 were similar at pH = 5.0, their profiles diverged markedly at pH = 7.0.

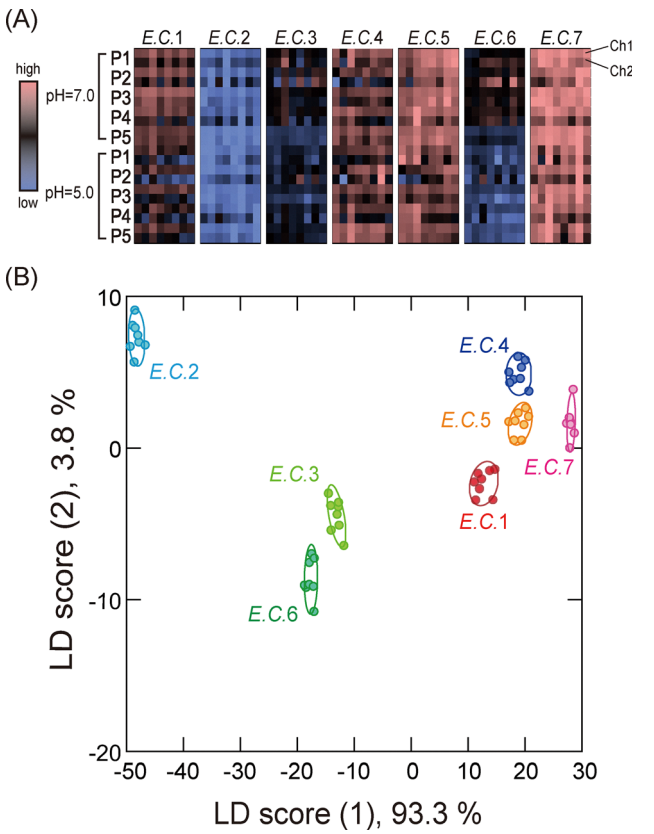

Fig. 3 Optical-pattern recognition of *E. coli* strains. (A) Heatmap of the fluorescence-response patterns for the seven different *E. coli* strains (OD_{600} = 0.10). Eight independent experimental values are shown for each analyte. (B) LDA score plot for the *E. coli* strains (OD_{600} = 0.10); ellipsoids represent confidence intervals (±1 SD) for each analyte.

To gain a more detailed understanding of the fluorescence-response patterns and evaluate their discrimination potential, the data were subjected to linear discriminant analysis (LDA). LDA is a supervised pattern-recognition algorithm that identifies projection directions maximizing the separation between classes while minimizing within-class variance, thus enabling visualization of complex multivariate data in a low-dimensional space. In the resulting discrimination score plot (Fig. 3B), the horizontal and vertical axes represent the first and second discriminant functions, respectively, that provide the greatest separation between classes (*i.e.*, bacterial strains). The clear separation of the clusters indicates that our Dnc-polymers can recognize the phenotypic differences among *E. coli* strains. The contributions of individual features were summarized using the standardized LDA coefficients, as shown in Table S1.

To quantitatively evaluate the discrimination performance of the fluorescence-pattern set, leave-one-out (LOO) cross-validation was performed. The LOO cross-validation is a model validation technique in which one pattern is omitted from the test data while the remaining data are used to train the model. This process is repeated for each pattern to comprehensively evaluate the discrimination accuracy. The LOO cross-validation yielded a discrimination accuracy of 98% (Fig. S3), demonstrating high accuracy in strain-level identification.

The *E. coli* strains selected in this study are commonly used in genetic-engineering experiments. In the discrimination-score plot, a clear separation was observed between the ΔOmpT strains (deficient in the outer membrane protease OmpT; *E.C.*2, *E.C.*3 and *E.C.*6) and non-deficient strains (*E.C.*1, *E.C.*4, *E.C.*5, and *E.C.*7) (Fig. 3B). This separation may be associated with differences in cell-surface characteristics arising from OmpT deficiency; however, this interpretation represents only one of several possibilities. The underlying mechanisms behind these observations will be investigated in detail in future studies. Such surface alterations are often subtle and are typically investigated by advanced techniques such as electron microscopy[44,45] or mass spectrometry,[46,47] which aim at direct structural or molecular characterizations. In contrast, our chemical-tongue strategy does not seek to explicitly resolve specific molecular features but instead exploits non-specific polymer–bacteria interactions to generate fluorescence response patterns, thereby enabling a simple and rapid discrimination of strain-dependent variations in bacterial surfaces.

Identification of *E. coli* strains in contaminated milk

Milk, as an animal-derived food product, is inherently susceptible to microbial contamination. Although thermal pasteurization is commonly used in milk processing, microbial contamination can occur post-pasteurization or *via* secondary contamination during handling. Commercially distributed milk often harbors lactic-acid bacteria and psychrotrophic bacteria (*e.g.*, *Pseudomonas*

spp. and *Acinetobacter* spp.) contamination,[48] which contribute to milk spoilage.[38] Although these bacteria can affect product quality, their presence is tolerated up to certain limits in many countries (*e.g.*, $<100\,000$ CFU mL^{-1} for raw milk or $<20\,000$ CFU mL^{-1} for pasteurized milk in the USA).[49] In contrast, permissible levels of pathogenic bacteria, such as *E. coli*, *Staphylococcus aureus*, and *Salmonella* spp., are strictly regulated worldwide; nevertheless, outbreaks continue to occur frequently and remain a major public health concern in the food sector.[6,7,39] Accordingly, there is a growing demand for technologies capable of both detecting and identifying bacterial strains, regardless of their pathogenicity, to improve public health.[38] With these considerations in mind, we next sought to detect milk-borne bacteria.

One major challenge in microbial detection in milk is the so-called masking effect, in which signals from the target bacteria are obscured by the abundant milk components. In particular, milk contains high concentrations of proteins (approximately 3.2–3.5%), which can lead to significant interference. Casein, which accounts for ~80% of milk protein,[50] forms micelles in milk through complexation with calcium and phosphate ions.[51] These colloidal particles are highly negatively charged and possess hydrophobic regions,[51] enabling them to encapsulate a variety of molecules.[52] This presents a concern for our Dnc-polymer-based chemical tongue, which relies on non-specific interactions; the presence of casein may lead to increased background fluorescence and, consequently, reduced sensitivity and accuracy. Therefore, efficient separation of bacteria from casein micelles is critical for a reliable microbial analysis in milk.

Filtration is an established method for microbial isolation, but tends to trap both bacteria and colloids.[53] We therefore exploited the fact that casein micelles can be dissolved by weakening their electrostatic interaction, which is achievable by the adjusting the pH to a mildly acidic value near the isoelectric point of casein (pI = 4.6)[54] and adding salts to induce electrostatic shielding.[55,56] Based on this principle, we developed a simple, selective pretreatment to recover bacterial cells from milk prior to chemical-tongue sensing.

Initially, we centrifuged the milk samples and then resuspended the pellet in distilled water; this process was repeated four times. However, when these samples were mixed with the Dnc-polymers, the fluorescence response was saturated at a small sample volume even in the absence of *E. coli* ('untreated' in Fig. 4A). This result indicates that co-precipitated milk components dominated the fluorescence signal, thereby masking any bacterial information. To address this issue, we screened various pretreatment conditions and found that adjusting the sample to 50 mM MES (pH = 5.7) containing 200 mM NaCl prior to centrifugation markedly reduced the pellet volume (Fig. 4B, 4C, and Fig. S4; for other conditions and a detailed interpretation of the results, see the SI). The OD_{600} of milk was reduced from above the measurable range (>10) to 0.024 through the pretreatment, corresponding to a substantial reduction in turbidity. When the pretreated samples were mixed with the Dnc-polymer panel, the milk-only sample showed decreased response ('treated' in Fig. 4A), suggesting effective removal of the colloidal milk components. In contrast, milk spiked with *E. coli* at ≥ 5 vol% (*i.e.*, $OD_{600} = 0.05$) exhibited clear bacteria-derived signals (Fig. 4A). These observations suggest that milk-derived components, particularly casein micelles and associated colloidal structures, generate nonspecific fluorescence responses that interfere with polymer–bacteria interactions. Therefore, the selective removal of these components is considered essential for achieving reliable strain discrimination in milk-based systems. As this pretreatment does not involve any complicated operations and demonstrates high reproducibility (Fig. S5), it is well suited for constructing a simple, nonspecific-interaction-based chemical-tongue platform for detecting milk-borne bacteria.

After processing milk samples contaminated with *E. coli* strains using the optimized pretreatment, we collected fluorescence-response patterns using the Dnc-polymers (Fig. S6 and Dataset S2), and an LDA was performed. The results showed that each strain forms a distinct cluster with no apparent overlap, and the control (milk without *E. coli*) formed its own cluster (Fig. 4D), confirming the effectiveness of the pretreatment. In addition, LOO cross validation yielded a classification accuracy of 100% (Fig. S7), demonstrating that our chemical tongue can reliably discriminate *E. coli* strains even in a complex matrix such as milk. It should be noted here that the pretreatment may introduce strain-dependent effects related to tolerance against acidic and high-salt conditions. Such biases, however, are inherent to preprocessing-based sensing strategies and do not invalidate the comparative discrimination demonstrated here.

In the practical microbial testing of milk, not only the identification of bacteria, but also the quantification of its abundance, is of critical importance. To address this, we selected two *E. coli* strains, *i.e.*, *E.C.*1 and *E.C.*5, that exhibited distinct fluorescence responses as model samples and evaluated their detectability in milk with varying contamination levels. Specifically, milk was spiked with either *E.C.*1 or *E.C.*5 at $OD_{600} = 0.08$, 0.16 or 0.24, or with a 1 : 1 mixture of the two strains ($OD_{600} = 0.12$ each). These samples were then subjected to the pretreatment protocol, and their corresponding fluorescence-response patterns were analyzed (Fig. S8 and Dataset S3). In the resulting discrimination plot (Fig. 4E), the clusters corresponding to each contamination level were clearly separated with no overlap, and the LOO cross-validation achieved 100% accuracy (Fig. S9). Notably, for both *E.C.*1 and *E.C.*5, the first discriminant score increased positively with increasing concentration, whereas the second discriminant score showed irregular variations at $OD_{600} = 0.08$, possibly due to interactions between residual milk components and the bacterial cells. For reference, when strain *E.C.*5 was examined separately, the practical lower concentration limit for reliable discrimination based on LOO cross-validation was estimated to be $OD_{600} \approx 0.025$–0.050 (Fig. S10).

Application to spoilage-associated bacteria

Next, we examined the applicability of our system to psychrotrophic bacteria that are frequently implicated in milk spoilage. As a representative spoilage-associated microorganism detected in raw milk, we focused on *Acinetobacter* spp., which are well known for their ability to grow at low temperatures.[48] In this

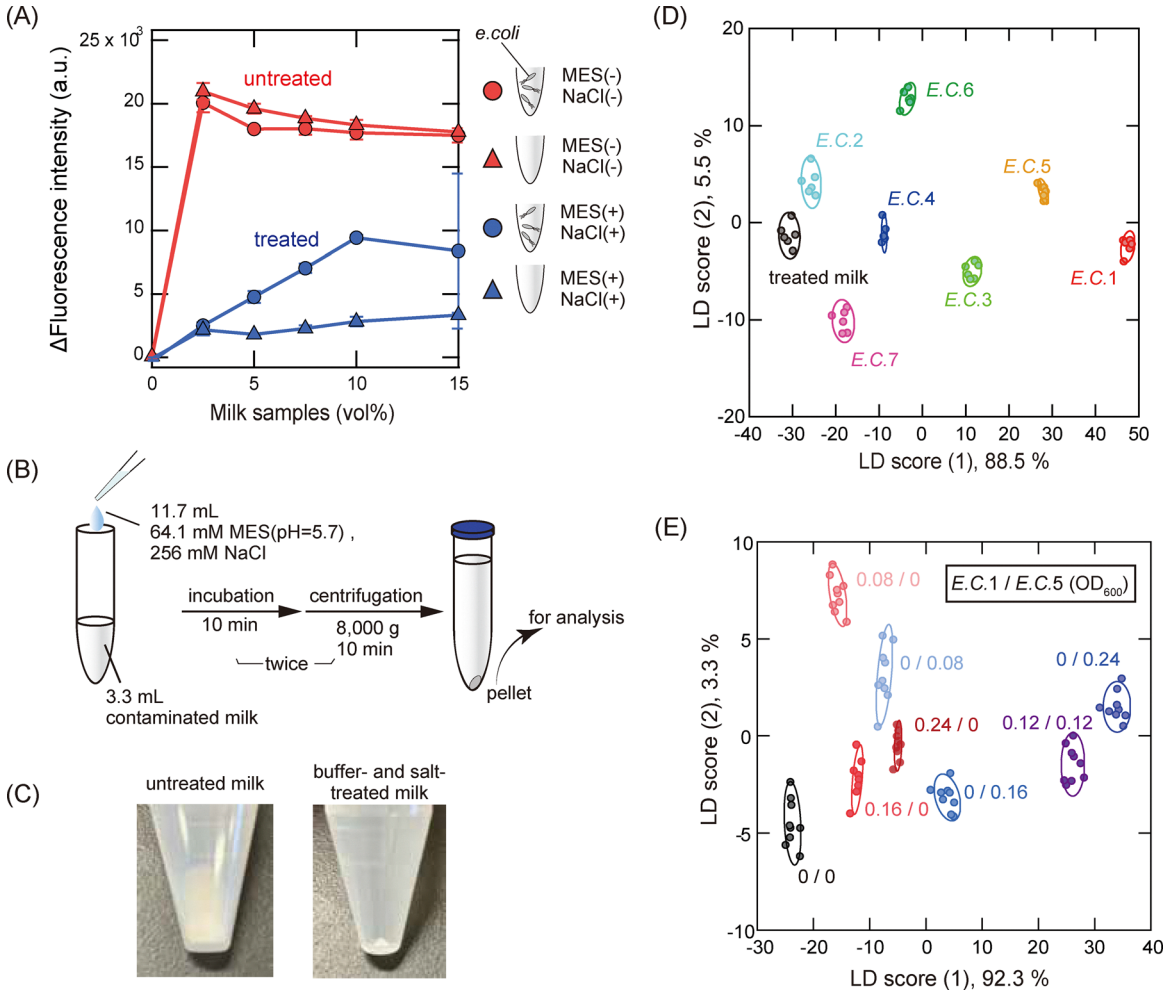

Fig. 4 Optical-pattern recognition of *E. coli* in contaminated milk. (A) Differences in the polymer-fluorescence response with/without pretreatment. Milk samples with/without *E.C.*3 were pretreated under the conditions shown on the right and then added to 20 μg mL^{-1} **P2** in 20 mM Acetate (pH = 5.0); $\lambda_{ex}/\lambda_{em}$ = 360 nm/530 nm; values shown represent mean values ±1 SE from three independent experiments. (B) Schematic of the pretreatment of milk contaminated with *E. coli*. (C) Photographs of collected samples with/without colloidal-particle-dispersion-buffer treatment. (D) and (E) LDA score plots for milk samples contaminated with *E. coli*: (D) seven different *E. coli* strains (OD_{600} = 0.1) and (E) mixtures of *E.C.*1 and/or *E.C.*5 (total OD_{600} = 0.08, 0.16, 0.24); ellipsoids represent confidence intervals (±1 SD) for each analyte.

study, an *A.B.* strain previously reported to be present in raw milk was selected as a model organism.[57]

The Dnc-polymers exhibited concentration-dependent turn-on fluorescence responses toward *A.B.* in buffer solutions (Fig. S11). Importantly, even in milk matrices, the established pretreatment procedure enabled the polymer-based chemical tongue to discriminate different levels of *A.B.* contamination (Fig. S12). Under these conditions, the discrimination limit was estimated to lie between $OD_{600} \approx 0.025$ and 0.050. These results indicate that the present sensing strategy is not limited to *E. coli*, but is also applicable to psychrotrophic spoilage-related bacteria relevant to milk quality.

We next investigated whether *E. coli* contamination and strain identity could be detected in the presence of *A.B.* As shown in Fig. 5A and Fig. S13 and Dataset S4, accurate identification of *E. coli* strains was achieved even when *A.B.* was present at a comparable concentration. Although the bacterial concentrations employed here are higher than those typically permitted in commercial milk (OD_{600} = 0.1 corresponds to 3.4 × 10^7 CFU mL^{-1} under our experimental conditions), these results demonstrate the potential of the system to distinguish *E. coli* from spoilage-associated bacteria under mixed conditions. Further optimization of probe design and measurement conditions may enable extension toward lower concentration regimes.

From a food-quality and safety perspective, it is also desirable to track how milk quality changes in response to the growth of spoilage-associated bacteria, even at levels that do not immediately cause visible spoilage. To explore this capability, milk samples were spiked with a relatively low concentration of *A.B.* (OD_{600} = 0.001, corresponding to 3.4 × 10^5 CFU mL^{-1} under our experimental conditions) and incubated statically at 30 °C as a model condition to accelerate spoilage-related changes.

The LDA score plot revealed that milk samples incubated without bacterial contamination exhibited minimal changes in cluster position over time (Fig. 5B and Dataset S5). In contrast, samples containing *A.B.* showed a pronounced time-dependent

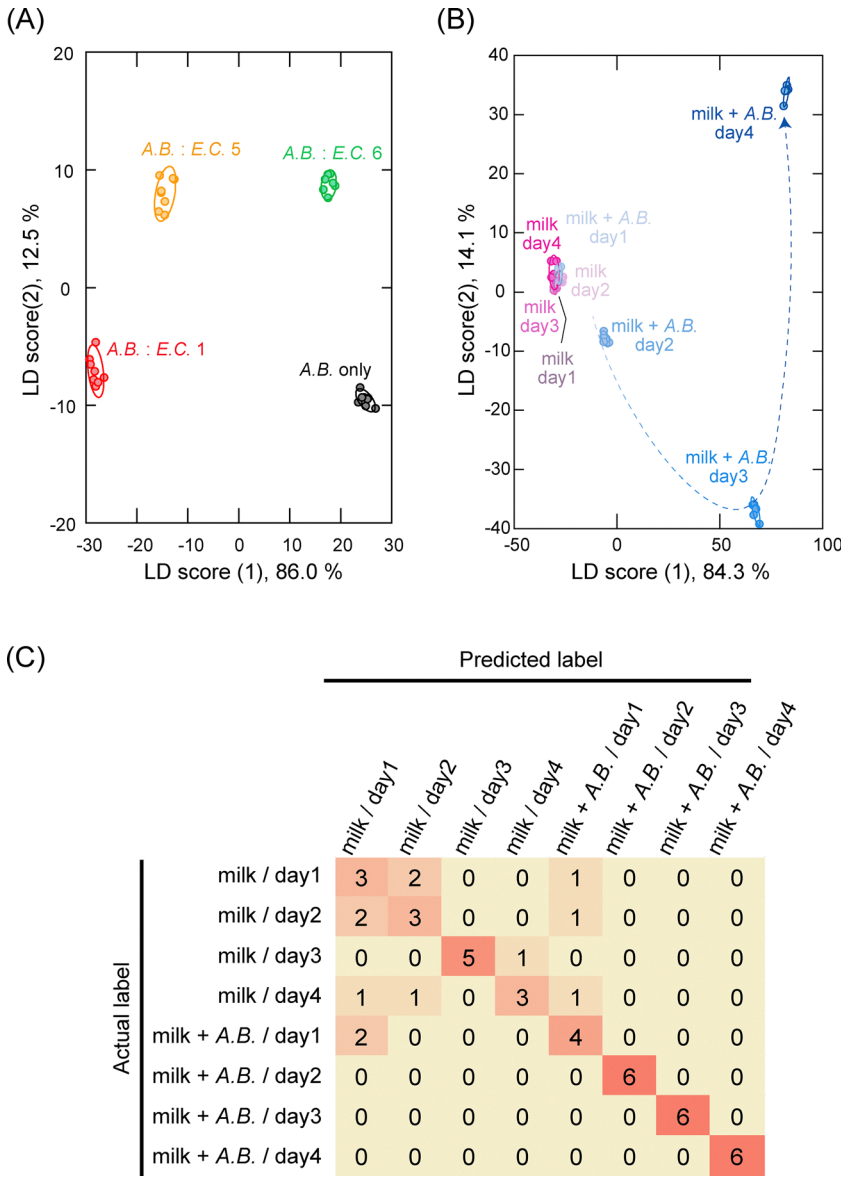

Fig. 5 Application of the chemical-tongue system to spoilage-associated bacteria in milk. (A) LDA score plot for samples containing a mixture of *A.B.* (OD_{600} = 0.1) and/or three individual *E. coli* strains (OD_{600} = 0.1); ellipsoids represent confidence intervals (±1 SD) for each analyte. (B) Time-course monitoring of milk spoilage caused by *A.B.* contamination. Milk samples with or without *A.B.* (OD_{600} = 0.001) were incubated at 30 °C and collected daily. Shown is the LDA score plot for milk samples with or without *A.B.*; ellipsoids represent confidence intervals (±1 SD) for each analyte. (C) Confusion matrix derived from an LOO cross-validation for the samples shown in (B); numbers indicate the number of samples assigned to each class.

shift in cluster position, *i.e.*, immediately after spiking, the samples overlapped with uncontaminated milk, whereas clear separation emerged as incubation proceeded. An LOO cross-validation further demonstrated that samples collected immediately after spiking could not be reliably distinguished from uncontaminated milk, while samples collected after one or more days of incubation were classified with 100% accuracy according to incubation time (Fig. 5C).

These results suggest that the proposed chemical-tongue system can capture time-dependent changes in milk quality initiated by contamination with spoilage-associated bacteria. This capability highlights the potential utility of the system for the practical monitoring of milk freshness and spoilage progression, thereby complementing its application to strain-level bacterial discrimination in food-quality-related contexts.

Generality, limitations, and future perspectives of the system

The polymer-based chemical-tongue system developed in this study, which incorporates the selective removal of milk-derived components, enables the detection, discrimination, and monitoring of *E. coli* strains and spoilage-associated bacteria in milk. To further evaluate the robustness and generality of the system with respect to matrix-related variability, we investigated the effects of day-to-day measurement variation, milk-lot differences, product brands, and fat content on the analytical performance. Specifically, five representative milk matrices

were examined: (i) the reference milk sample used throughout this study, (ii) the same milk sample measured on a different day to assess day-to-day measurement variation, (iii) milk from a different production lot of the same brand, (iv) milk from a different manufacturer, and (v) low-fat milk. Each milk matrix was spiked with three microbial strains (*E.C.*1, *E.C.*5, and *A.B.*; OD_{600} = 0.1) and analyzed under otherwise identical conditions.

The resulting LDA score plot revealed the formation of distinct subclusters corresponding to each microbial strain, regardless of the milk matrix used (Fig. 6 and Dataset S6). This observation indicates that the established pretreatment effectively suppresses the influence of milk-derived components and minimizes matrix-dependent variations. To further examine the generality of the system, fluorescence-response patterns obtained from the reference milk matrix (i) were used as training data, and the discrimination of bacterial strains spiked into the remaining milk matrices (ii–v) was evaluated using a holdout test. Classification performance was assessed using predefined feature subsets (all variables, Ch1 only, Ch2 only, pH = 7.0 only, or pH = 5.0 only). While the classification accuracies varied depending on the feature subset used (approximately 83–97%), discriminative information was largely preserved across different conditions (Dataset S6). Notably, misclassifications observed in the holdout tests did not concentrate on a specific milk matrix, suggesting that the errors were not primarily driven by matrix-specific effects but rather by intrinsic similarities among certain strains.

However, in addition to matrix-related variability, the robustness of the classification model to biological variation should be considered. In the present study, bacterial samples were prepared under standardized culture conditions to reduce potential variability. Nevertheless, systematic evaluation of batch-to-batch variation, growth phases or environmental stress effects was not performed and remains an important subject for future investigation. Furthermore, as the system relies on supervised learning, misclassification may occur when encountering closely related strains not included in the training set. Expanding the training library and incorporating a broader range of strains will be essential to improve generalizability and scalability.

Despite this robustness, limitations in sensitivity remain. The current discrimination limit of the system is $OD_{600} \approx 0.025$–0.050 (Fig. S10 and S12), which corresponds to $\sim 10^7$ CFU mL^{-1} for the microorganisms examined under the applied conditions. This level exceeds the permissible total bacterial count for pasteurized milk in the USA.[49] In addition, *E. coli* contamination in milk is strictly regulated due to concerns over fecal contamination (*e.g.*, <10 CFU mL^{-1} for pasteurized milk in the USA).[49] Therefore, the sensitivity of the present method does not yet meet current regulatory thresholds. Although future improvements such as enhancing probe-binding affinity, optimizing the fluorophores, and incorporating signal-amplification mechanisms may enhance sensitivity, further investigation will be required to determine whether detection at regulatory levels can be achieved. In practical settings where pre-enrichment is acceptable, samples containing lower initial bacterial loads may become detectable after enrichment, potentially extending the practical applicability of the system.

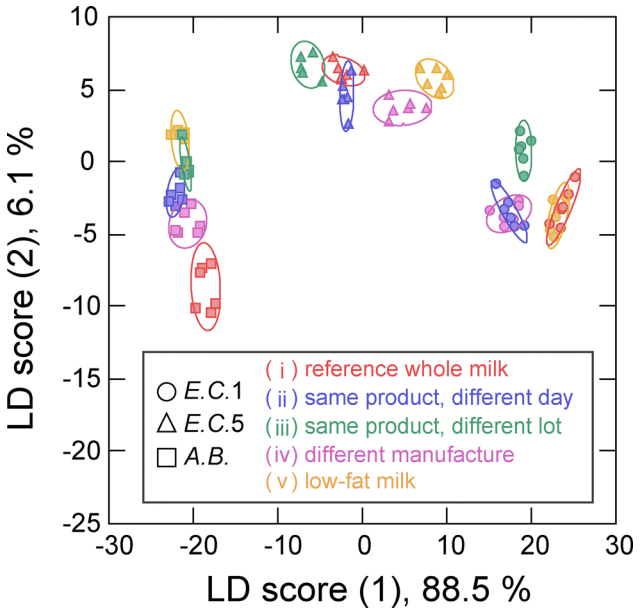

Fig. 6 Robustness of the chemical-tongue system against variations in milk matrices. LDA score plot for milk samples spiked with three microbial strains (*E.C.*1, *E.C.*5, and *A.B.*; OD_{600} = 0.1) across five different milk matrices. The matrices include: (i) the reference whole milk used throughout this study, (ii) the same product measured on a different day, (iii) a different production lot of the same product, (iv) whole milk from a different manufacturer, and (v) low-fat milk; ellipsoids represent confidence intervals (±1 SD) for each analyte.

Importantly, we have demonstrated that the system can detect time-dependent quality changes in milk initiated by the presence of low levels of spoilage-associated bacteria (Fig. 6). Even when the initial bacterial concentration was below the discrimination limit, progressive changes in fluorescence-response patterns were observed with increasing bacterial growth during incubation. From a practical standpoint, this time-resolved monitoring capability is highly relevant to food-quality management, as it allows early detection of spoilage progression rather than relying solely on absolute bacterial counts.

Overall, the present chemical-tongue system enables a strain-level discrimination of bacteria in milk, which has hitherto been challenging for conventional approaches, while also allowing the monitoring of contamination-induced quality changes. Previous studies have applied chemical-tongue strategies to milk-borne bacteria,[34,35,58,59] typically by analyzing unprocessed milk[35,58] or by identifying individual species or their mixtures using simple centrifugation followed by pellet resuspension[34] and additional filtration steps.[55] To place the present approach in the context of existing technologies, a comparative overview of representative PCR- and sensor-array–based methods for bacterial analysis in milk is provided in Table S3. Molecular techniques such as PCR offer high analytical sensitivity and target specificity, and advanced genomic methods (*e.g.*, whole-genome sequencing) can provide strain-level resolution. However, these approaches often require DNA extraction, specialized instrumentation, and relatively time-consuming workflows. In contrast, the present chemical-tongue system prioritizes rapid,

cultivation-free strain discrimination and operational simplicity over ultra-trace detection. Moreover, the polymer probes used in this study can be synthesized through straightforward procedures (see the SI for details) in small quantities and typically in high isolated yields. Because only microgram-level amounts are required per assay (on the order of $\mu g\ mL^{-1}$ in total reaction volumes of several tens to hundreds of microliters), the material cost per measurement is negligible relative to standard laboratory consumables, supporting the practical and cost-effective nature of the platform.

Although the present strategy cannot identify unknown *E. coli* strains without prior training, it can accurately recognize any strains included in the training set. Furthermore, this approach is likely extendable to broader taxonomic levels such as species or genera, for which phenotypic differences are expected to be more pronounced. While further investigations are required to determine whether this system can detect trace levels of pathogenic strains, the developments presented herein can be expected to eventually lead to the establishment of a practical sensing platform for improving food safety and -quality control.

Conclusion

In summary, we have developed a polymer-based chemical tongue that enables reliable, qualitative strain-level discrimination of *E. coli* strains based on fluorescence-response patterns generated through non-specific polymer–bacteria interactions. By integrating a simple cell-separation process tailored to the complex milk matrix, our system retains discriminative capability even in the presence of abundant interfering components. Such minimal sample pretreatment represents an effective strategy in chemical-tongue sensing, which inherently relies on matrix-sensitive, non-specific interactions. While the present system does not yet achieve detection limits required for regulatory rule-out of pathogenic *E. coli*, it provides a practical framework for rapid screening of high-level contamination and spoilage-associated bacteria in milk. Microbial contamination also poses risks in other food products (*e.g.*, raw meat, seafood, and vegetables); however, the distinct composition of these matrices would require tailored pretreatment strategies. Accordingly, although systematic optimization will be necessary for implementation beyond milk, the conceptual framework presented here offers a foundation for developing adaptable microbial screening platforms across diverse food products.

Author contributions

Conceptualization: K. T., H. K., and S. T; data curation, investigation, and formal analysis: K. T; funding acquisition: S. T; resources: H. K., H. T., R. K., and S. T.; methodology, visualization, and writing – original draft: K. T. and S. T.; supervision: H. T., R. K., and S. T.; writing – review & editing: all authors.

Conflicts of interest

There are no conflicts to declare.

Data availability

The data supporting this article have been included as part of the supplementary information (SI). The SI contains detailed synthetic procedures; Fig. S1–S13 presenting the binding isotherms of Dnc-polymers; confusion matrices; screening of preprocessing conditions; fluorescence-response heatmaps under various conditions; LDA score plots; Tables S1–S3; and legends for the SI datasets. See DOI: https://doi.org/10.1039/d5tb01573a.

Acknowledgements

This work was partially supported by JST FOREST Program, Grant Number JPMJFR233R (to S. T.) and JSPS KAKENHI grant JP20H02774 (to S. T.). The authors thank Sayaka Ishihara and Naoko Kitogo (Health and Medical Research Institute, AIST) for their valuable technical assistance and experimental support.

References

1 M. M. Abedin, R. Chourasia, L. C. Phukon, P. Sarkar, R. C. Ray, S. P. Singh and A. K. Rai, *Crit. Rev. Food Sci. Nutr.*, 2024, **64**, 10730–10748.
2 J. V. Pham, M. A. Yilma, A. Feliz, M. T. Majid, N. Maffetone, J. R. Walker, E. Kim, H. J. Cho, J. M. Reynolds, M. C. Song, S. R. Park and Y. J. Yoon, *Front. Microbiol.*, 2019, **10**, 1404.
3 J. F. Prescott, A. N. Rycroft, J. D. Boyce, J. I. MacInnes, F. Van Immerseel and J. A. Vázquez-Boland, *Pathogenesis of Bacterial Infections in Animals*, Wiley-Blackwell, 2022.
4 R. C. Nnachi, N. Sui, B. Ke, Z. Luo, N. Bhalla, D. He and Z. Yang, *Environ. Int.*, 2022, **166**, 107357.
5 G. Ekici and E. Dümen, in *The Universe of Escherichia coli*, ed M. S. Erjavec, IntechOpen, 2019, ch. 5, pp. 85–100.
6 K. E. Heiman, R. K. Mody, S. D. Johnson, P. M. Griffin and L. H. Gould, *Emerging Infect. Dis.*, 2015, **21**, 1293–1301.
7 S. Hirose, K. Ohya, T. Yoshinari, T. Ohnishi, K. Mizukami, T. Suzuki, K. Takinami, T. Suzuki, K. Lee, S. Iyoda, Y. Akeda, Y. Yahata, Y. Tsuchihashi, T. Sunagawa and Y. Hara-Kudo, *Epidemiol. Infect.*, 2023, **151**, e150.
8 L. Váradi, J. L. Luo, D. E. Hibbs, J. D. Perry, R. J. Anderson, S. Orenga and P. W. Groundwater, *Chem. Soc. Rev.*, 2017, **46**, 4818–4832.
9 A. Samantaray, S. Chattaraj, D. Mitra, A. Ganguly, R. Kumar, A. Gaur, P. K. D. Mohapatra, S. de, L. Santos-Villalobos, A. Rani and H. Thatoi, *Curr. Res. Microb. Sci.*, 2024, **7**, 100251.
10 S. Tokonami and T. Iida, *Anal. Chim. Acta*, 2017, **988**, 1–16.
11 J. S. Johnson, D. J. Spakowicz, B.-Y. Hong, L. M. Petersen, P. Demkowicz, L. Chen, S. R. Leopold, B. M. Hanson, H. O. Agresta, M. Gerstein, E. Sodergren and G. M. Weinstock, *Nat. Commun.*, 2019, **10**, 5029.
12 A. Haider, M. Ringer, Z. Kotroczó, C. Mohácsi-Farkas and T. Kocsis, *Microbiol. Res.*, 2023, **14**, 80–90.

13 Y. Geng, W. J. Peveler and V. M. Rotello, *Angew. Chem., Int. Ed.*, 2019, **58**, 5190–5200.
14 Z.-H. Chen, Q.-X. Fan, X.-Y. Han, G. Shi and M. Zhang, *Trends Analyt. Chem.*, 2020, **124**, 115794.
15 S. Tomita and H. Sugai, *Biophys. Physicobiol.*, 2024, **21**, e210017.
16 C. W. Smith, M. S. Hizir, N. Nandu and M. V. Yigit, *Anal. Chem.*, 2022, **94**, 1195–1202.
17 H. Sugai, S. Tomita, S. Ishihara, K. Shiraki and R. Kurita, *Chem. Commun.*, 2022, **58**, 11083–11086.
18 X.-Y. Hu, Z.-Y. Hu, J.-H. Tian, L. Shi, F. Ding, H.-B. Li and D.-S. Guo, *Chem. Commun.*, 2022, **58**, 13198–13201.
19 X. Wang, R. Xu, Y. Wang, M. Li, H. Wei, G. Qin, Y. Li and Y. Wei, *Talanta*, 2025, **288**, 127727.
20 Q.-Y. Li, L. Ma, L. Li, S. Wang, X. Li, C. Zhang, Y. Zhang, M. Jiang, H. Wang, K. Huang, X. Yu and L. Xu, *Chem. Eng. J.*, 2022, **430**, 132696.
21 R. Mungkarndee, I. Techakriengkrai, G. Tumcharern and M. Sukwattanasinitt, *Food Chem.*, 2016, **197**, 198–204.
22 M. Jia, Y. Pan, J. Zhou and M. Zhang, *Food Chem.*, 2021, **335**, 127566.
23 Y. Yu, F. Shi, Y. Zhang, F. Li and J. Han, *J. Future Foods*, 2024, **4**, 48–60.
24 C. Yang, Y. Xiao, Y. Yan and H. Zhang, *Anal. Methods*, 2025, **17**, 525–532.
25 B. Li, X. Li, Y. Dong, B. Wang, D. Li, Y. Shi and Y. Wu, *Anal. Chem.*, 2017, **89**, 10639–10643.
26 S. Chen, L. Wei, X.-W. Chen and J.-H. Wang, *Anal. Chem.*, 2015, **87**, 10902–10909.
27 W. Chen, Q. Li, W. Zheng, F. Hu, G. Zhang, Z. Wang, D. Zhang and X. Jiang, *Angew. Chem., Int. Ed.*, 2014, **53**, 13954–13959.
28 R. L. Phillips, O. R. Miranda, C.-C. You, V. M. Rotello and U. H. F. Bunz, *Angew. Chem., Int. Ed.*, 2008, **47**, 2590–2594.
29 A. Laliwala, A. Pant, D. Svechkarev, M. R. Sadykov and A. M. Mohs, *NPJ Biosens.*, 2024, **1**, 17.
30 C. Yang and H. Zhang, *Microchim. Acta*, 2023, **190**, 451.
31 A. Laliwala, R. Gupta, D. Svechkarev, K. W. Bayles, M. R. Sadykov and A. M. Mohs, *Microchem. J.*, 2024, **206**, 111395.
32 Z. Liu, X. Zhu, Q. Lu, M. Liu, H. Li, Y. Zhang, Y. Liu and S. Yao, *Anal. Chem.*, 2023, **95**, 5911–5919.
33 S. Tomita, H. Kusada, N. Kojima, S. Ishihara, K. Miyazaki, H. Tamaki and R. Kurita, *Chem. Sci.*, 2022, **13**, 5830–5837.
34 Y. Qin, J. Sun, W. Huang, H. Yue, F. Meng and M. Zhang, *Food Chem. X*, 2024, **22**, 101281.
35 H. Li, S. Yao, X. Wang, H. Xu, C. Zhao, J. Li and J. Wang, *Microchem. J.*, 2024, **197**, 109719.
36 M. Xiao, L. Mei, J. Qi, L. Zhu and F. Wang, *Microchem. J.*, 2024, **201**, 110701.
37 Y. Zhang, C. Zhao, K. Zheng, H. Li, T. Yang, F. Hu, J. Zhang, X. Huang, Z. Li, J. Shi, Z. Guo, S. Gao and X. Zou, *Anal. Chem.*, 2025, **97**, 9848–9857.
38 V. Fusco, D. Chieffi, F. Fanelli, A. F. Logrieco, G.-S. Cho, J. Kabisch, C. Böhnlein and C. M. A. P. Franz, *Compr. Rev. Food Sci. Food Saf.*, 2020, **19**, 2013–2049.
39 S.-C. Yang, C.-H. Lin, I. A. Aljuffali and J.-Y. Fang, *Arch. Microbiol.*, 2017, **199**, 811–825.
40 S. Tomita, S. Ishihara and R. Kurita, *J. Mater. Chem. B*, 2022, **37**, 7581–7590.
41 S. Tomita, S. Ishihara and R. Kurita, *ACS Appl. Mater. Interfaces*, 2017, **9**, 22970–22976.
42 H. Sugai, S. Tomita, S. Ishihara and R. Kurita, *ACS Sens.*, 2019, **4**, 827–831.
43 X. Qin, X. Yang, K. Du and M. Li, *RSC Med. Chem.*, 2021, **12**, 1826–1838.
44 M. S. I. Khan, S.-W. Oh and Y.-J. Kim, *Sci. Rep.*, 2020, **10**, 2368.
45 A. Hisada, E. Matsumoto, R. Hirano, M. Konomi, J. Y. Bou Khalil, D. Raoult and Y. Ominami, *Sci. Rep.*, 2023, **13**, 11258.
46 X.-F. Chen, X. Hou, M. Xiao, L. Zhang, J.-W. Cheng, M.-L. Zhou, J.-J. Huang, J.-J. Zhang, Y.-C. Xu and P.-R. Hsueh, *Microorganisms*, 2021, **9**, 1536.
47 V. Pereira, P. Abraham, S. Nallapeta and A. Shetty, *BMC Gastroenterol.*, 2018, **18**, 20.
48 L. Quigley, O. O'Sullivan, C. Stanton, T. P. Beresford, R. P. Ross, G. F. Fitzgerald and P. D. Cotter, *FEMS Microbiol. Rev.*, 2013, **37**, 664–698.
49 2023 Revision Grade "A" Pasteurized Milk Ordinance (PMO), Public Health Service/Food and Drug Administration, https://www.fda.gov/media/180975/download?attachment, (accessed June 2025).
50 D. Roy, A. Ye, P. J. Moughan and H. Singh, *Front. Nutr.*, 2020, **7**, 577759.
51 D. J. McMahon and R. J. Brown, *J. Dairy Sci.*, 1984, **67**, 499–512.
52 F. Rehan, N. Ahemad and M. Gupta, *Colloids Surf., B*, 2019, **179**, 280–292.
53 G. Panopoulos, G. Moatsou, C. Psychogyiopoulou and E. Moschopoulou, *Foods*, 2020, **9**, 284.
54 Y. Liu and R. Guo, *Biophys. Chem.*, 2008, **136**, 67–73.
55 T. Huppertz and P. F. Fox, *Int. Dairy J.*, 2006, **16**, 1142–1148.
56 Z. Zhao and M. Corredig, *J. Dairy Sci.*, 2016, **99**, 6036–6045.
57 H. M. A. Mohamed, H. H. Abd-Elhafeez, O. A. Al-Jabr and M. A. El-Zamkan, *Biology*, 2022, **11**, 1845.
58 Y. Wang, Y. Feng, Z. Xiao and Y. Luo, *Food Chem.*, 2025, **463**, 141115.
59 X. Han, L. Che, Y. Zhao, Y. Chen, S. Zhou, J. Wang, M. Yin, S. Wang and Q. Deng, *Sens. Actuators, B*, 2023, **388**, 133847.